remote sensing

MDPI

Technical Note

A Smart Noise Jamming Suppression Method Based on Atomic Dictionary Parameter Optimization Decomposition

Zhidong Liu [1,2,*], Qun Zhang [1,2,3] and Kaiming Li [1,2]

[1] Information and Navigation College, Air Force Engineering University, Xi'an 710077, China; afeuzq@163.com (Q.Z.); likaiming1982@163.com (K.L.)
[2] The Collaborative Innovation Center of Information Sensing and Understanding, Xi'an 710077, China
[3] Key Laboratory of Wave Scattering and Remote Sensing Information, Fudan University, Shanghai 200433, China
* Correspondence: liuzd13@tsinghua.org.cn

Abstract: Smart noise jamming is a new jamming style against radar, which plays an important role in modern radar electronic warfare. In order to solve the complex problem of convolutional smart noise jamming suppression with different time delay and jamming frequency modulation, a novel jamming suppression method based on the optimized atomic dictionary decomposition by estimating significant jamming parameters is proposed in this paper. First, the dual channel jamming signal information is obtained by designing twinning waveforms, then the independent estimation of time delay and jamming frequency parameters are established based on the spatial position sequences of the false targets. After that, the atomic dictionary is optimized by utilizing the obtained jamming parameters to achieve more effective decomposition. The performance of the new jamming suppression method is analyzed and verified by experimental simulations. The results show that this method can feasibly and practicably suppress the smart noise jamming with a deceptive effect, and the atomic decomposition efficiency is highly improved.

Keywords: twinning waveform; atomic decomposition; smart noise jamming; jamming suppression

check for updates

Citation: Liu, Z.; Zhang, Q.; Li, K. A Smart Noise Jamming Suppression Method Based on Atomic Dictionary Parameter Optimization Decomposition. *Remote Sens.* **2022**, *14*, 1921. https://doi.org/10.3390/rs14081921

Academic Editor: Okan Yurduseven

Received: 22 March 2022
Accepted: 13 April 2022
Published: 15 April 2022

Publisher's Note: MDPI stays neutral with regard to jurisdictional claims in published maps and institutional affiliations.

Copyright: © 2022 by the authors. Licensee MDPI, Basel, Switzerland. This article is an open access article distributed under the terms and conditions of the Creative Commons Attribution (CC BY) license (https://creativecommons.org/licenses/by/4.0/).

1. Introduction

With the development of the digital radio frequency memory (DRFM) technique [1], a new flexible smart noise jamming method is designed against linear frequency modulated (LFM) radar, which is generated by the noise modulating the copy of the transmitted radar signal [2,3]. By dynamically adjusting the jamming time delay sequence and jamming frequency sequence in the copy of the transmitted radar signal, the spatial position of false targets can be moved. Therefore, smart noise jamming can realize blanket jamming and deception jamming simultaneously [4]. Smart noise jamming can effectively make use of the power of the target signal and increase the difficulty of jamming suppression by taking advantage of the random character of noise sequence [5].

The existing research on smart noise jamming suppression mainly focuses on jamming characteristic parameter extraction and anti-jamming signal waveform design. In [6], the fractional Fourier transform is used to extract jamming features to suppress jamming and achieve accurate extraction of true target positions. Based on orthogonal diversity technology, the waveform with fuzzy function sensitive to echo frequency is designed in [7], which achieves effective suppression of smart noise jamming. The smeared spectrum technology is used in [8] to accurately estimate the jamming characteristic parameters, while in [9] it is realized by establishing a mathematical model between the peak position of dense false targets and the transmitted signal parameters. In [10], a suppression method based on multi-dimensional feature joint processing is proposed to further improve the recognition and suppression performance of smart noise jamming. For the radar target detection task, the identification and suppression of different types of smart jamming is realized

through space-time adaptive processing in [11]. The above jamming suppression method requires the complex transformation processing of mixed signals after jamming, and the jamming suppression effect is greatly affected by the jamming to signal ratio (JSR) and other factors. In order to improve the performance of the above jamming suppression methods, new solutions need to be introduced, among which atomic decomposition technology is a promising one.

Atomic decomposition technology has great potential in radar signal processing and related applications [12]. In imaging applications, atomic decomposition is used to represent the Radar Cross Section (RSC) of the target, which can optimize the design of the transmitted waveform [13]. In [14], model-based atomic diversity imaging is proposed, which uses signal components to realize focused imaging step-by-step, and the adaptability of Synthetic Aperture Radar (SAR) imaging to the target geometry is improved. The problem of noise pollution in Inverse Synthetic Aperture Radar (ISAR) imaging can also be improved by atomic decomposition technique [15]. In the application of parameter estimation, the atomic decomposition algorithm based on subspace orthogonal matching pursuit technology can avoid the over-fitting phenomenon and the accuracy of parameter estimation is improved [16]. In order to solve the problem of signal detection and estimation in gaussian white noise background, the maximum likelihood estimation of mixed signals can be approximated by means of expectation maximization and atomic decomposition [17]. At the same time, atomic decomposition is often used in the signal sparse decomposition algorithm to solve the problem of feature extraction and transformation basis mismatch [18,19]. The sinusoidal factor in the atomic dictionary can be used to match and represent the nonlinear time-frequency signal, and the pulse-modulated signal can be sparsely represented more effectively [20].

Based on the advantages that atomic decomposition technology can achieve, including feature extraction and reconstruction of complex signals, some studies have applied it to the suppression of dense deception jamming [21–23]. In [22], the essential characteristics of real targets and dense false targets are effectively analyzed by combining Gabor transformation and time-frequency atomic decomposition theory. In [23], atomic decomposition theory is adopted to extract the difference features between the jamming signal and target signal and suppress smeared spectrum jamming. For the smart noise jamming to be suppressed in this paper, the efficiency of existing atomic decomposition methods is not satisfactory and the dictionary design is redundant. Further studies are needed to understand how to optimize the existing dictionary design and improve the performance of jamming suppression.

Therefore, in combination with the twinning waveform design [24], this paper proposes an optimal atomic decomposition suppression method based on jamming characteristic parameters. The parameters set by the atomic dictionary are optimized by the estimated jamming characteristic parameters, the target echo and smart noise signals are projected onto different atomic bases, and the jamming signals are separated and eliminated effectively.

The structure of this paper is as follows. The jamming signal model is established and the spatial position of false targets is presented in Section 2. Section 3 presents a method of jamming parameter estimation by twinning waveform in detail. In Section 4, anti-jamming simulations are presented in different dimensions and the validity of the proposed method is proved. Finally, conclusions are drawn in Section 5.

2. Jamming Signal Model

Without considering the RCS and other characteristics of the target, the transmitting signal is a LFM signal and we assume that its carrier frequency is zero, the bandwidth is B, the pulse width is T_p, and the chirp rate is K. Based on the above assumptions, the signal expression is as follows:

$$s(t) = rect\left(\frac{t}{T_p}\right)\exp\left(\mathrm{j}\pi K t^2\right) \tag{1}$$

where $rect\left(\hat{t}/T_p\right)$ yields 1 when $\left|\hat{t}/T_p\right| < 0.5$, and 0 otherwise.

Smart noise convolution jamming first intercepts the target signal $s(t)$, then the noise sequence ω_q is used to modulate it. The jamming signal is obtained by adding the jamming delay sequence τ_q, jamming frequency sequence f_q, and jamming phase ϕ_d, as shown in the following expression:

$$s_J(t) = \sqrt{P_J}\sum_{q=1}^{Q}\omega_q s(t-\tau_q, T)\exp\left[\mathrm{j}2\pi f_q(t-\tau_q)+\mathrm{j}\phi_d\right] \tag{2}$$

where P_J is the power of jammer, Q is the number of copies of the radar transmitted signal forwarded by jammer, and the energy of jamming signal is determined by the power of jammer and the number of copies together.

The jamming signal in the frequency domain obtained by Fourier transform is as follows.

$$s_J(f) = \sqrt{P_J}\exp(\mathrm{j}\phi_d)\cdot\sum_{q=1}^{Q}\omega_q s(f-f_q)\exp\left[-\mathrm{j}2\pi(f-f_q)\tau_q\right] \tag{3}$$

Matched filtering is used for imaging processing, and the results are as follows.

$$Y(f) = s_J(f)\cdot FT\left[s^*(T_p-t, T_p)\right] \tag{4}$$

The transmitted signal is substituted into Equation (4) to obtain the following expression:

$$Y(f) = \mathbb{C}\cdot\sum_{q=1}^{Q}\omega_q rect(f-f_q/2/B-f_q)\exp\left\{-\mathrm{j}\pi f_q^2/K\right\}\cdot\exp(-\mathrm{j}2\pi f_q\tau_q)\exp\left[-\mathrm{j}2\pi f\left(\tau_q-\frac{f_q}{K}\right)\right] \tag{5}$$

where $\mathbb{C} = \sqrt{P_j}\exp(\mathrm{j}\phi_d)$ is a constant. In combination with the noise sequence $\{\omega_q\}$, the mixed amplitude modulation coefficient $\mathbb{C}_q = \sqrt{P_j}\omega_q\exp(\mathrm{j}\phi_d)$ is defined and the corresponding amplitude modulation is performed on the copy of the forwarded radar signal, respectively. By the inverse Fourier transform, the time-domain imaging results are as follows.

$$Y(t) = \mathbb{C}\cdot\sum_{q=1}^{Q}\omega_q rect(f-f_q/2/B-f_q)\exp\left\{-\mathrm{j}\pi f_q^2/K\right\}\cdot\exp(-\mathrm{j}2\pi f_q\tau_q)\sin c\left[(B-f_q)\left(t-\tau_q+\frac{f_q}{K}\right)\right] \tag{6}$$

According to Equation (6), it can be obtained that the corresponding position of each peak output of the jamming of convolutional smart noise is as follows.

$$t_d(q) = t-\tau_q+\frac{f_q}{K} \tag{7}$$

According to Equation (7), it can be found that the spatial position of false targets generated by smart convolution jamming is jointly determined by the jamming delay sequence and jamming frequency. In order to achieve an accurate reconstruction of jamming signals, the accurate estimation of the jamming delay sequence $\{\tau_q\}$ and jamming frequency sequence $\{f_q\}$ should be achieved, respectively.

3. Jamming Parameter Estimation Method

Based on the jamming model analysis in Section 2, the accurate estimation of the two jamming characteristic parameters cannot be achieved only by detecting the peak position of the false target once, so the twinning waveform design is introduced.

Under the condition of sufficient radar resources and equipment conditions, a double pulse transmitting signal is designed to detect the peak position of two false targets, and the original under definite equation is changed into a positive definite equation. The independent estimation of jamming characteristic parameters is realized by supplementing a conditional equation.

Twinning Waveform Design

The traditional LFM signal and twinning waveform signal can be transmitted simultaneously in one transmission channel by designing different signal modulation frequencies in even and odd sampling sequences. We assume that the sampling frequency of the signal is f_s, the sampling period is T_s, and the total number of samples of the composite LFM waveform is

$$N = T_p / T_s \tag{8}$$

For the k-th signal sample, the sampling function is designed as follows.

$$\eta_k(t) = \mathrm{rect}\left(\frac{t - T_p/2 + kT_s}{T_s}\right),\ 0 \le k \le N \tag{9}$$

In order to obtain twinning waveform signals with similar structure but different chirp rates, it is necessary to design two groups of different signal bandwidths, B_1 and B_2, and calculate the corresponding chirp rates,$K_1 = 2B_1/T_p$ and $K_2 = 2B_2/T_p$.

When the number of sample sequences is odd, the expression of the traditional LFM signal $s_{2i-1}(t)$ is obtained by combining Equations (1) and (9).

$$s_{2i-1}(t) = \mathrm{rect}\left(\frac{t - T_p/2 + (2i-1)T_s}{T_s}\right)\exp\left(\mathrm{j}\pi K_1 t^2\right) \tag{10}$$

When the number of sample sequences is even, the expression of the twinning waveform signal $s_{2i}(t)$ is also obtained as follows:

$$s_{2i}(t) = \mathrm{rect}\left(\frac{t - T_p/2 + 2iT_s}{T_s}\right)\exp\left(\mathrm{j}\pi K_2 t^2\right) \tag{11}$$

where K_2 is the chirp rate of the twinning waveform. The expression of the composite LFM signal is as follows:

$$S_{twin}(t) = \sum_{i=1}^{m}\left(s_{2i-1}(t) + s_{2i}(t)\right) \tag{12}$$

where $m = \lfloor N/2 \rfloor$ and $\lfloor\rfloor$ means round down.

Figure 1 shows the instantaneous frequency of twinning waveform signals separated by odd-even sampling sequences. The abscissa t represents the signal's time domain and the ordinate $f(t)$ represents the signal's frequency domain distribution. The instantaneous frequency of the signal after the separation of the odd sampling sequence $f_o(t)$ is expressed as follows, which is as shown by the solid blue line in Figure 1.

$$f_o(t) = \mathrm{rect}\left(\frac{t}{T_p/2}\right)K_1 t = \mathrm{rect}\left(\frac{t}{T_p/2}\right)\frac{2B_1}{T_p}t \tag{13}$$

The instantaneous frequency of the signal after the separation of the even sampling sequence $f_e(t)$ is expressed as follows, which is as shown by the solid blue line in Figure 1.

$$f_e(t) = \mathrm{rect}\left(\frac{t}{T_p/2}\right)K_2 t = \mathrm{rect}\left(\frac{t}{T_p/2}\right)\frac{2B_2}{T_p}t \tag{14}$$

Based on the above design of twinning waveforms, two transmitted signals with different frequency modulation slopes can be obtained. After jamming, two jamming signals S_{J1} and S_{J2} can be obtained by separation and reorganization. Then, the reference signals of the two channels are combined to conduct imaging processing on the interfered signals to obtain two sets of jamming results. Finally, the peak value of the imaging results is detected to obtain the delay sequence, $\{t_{d1}(q)\}$ and $\{t_{d2}(q)\}$, corresponding to the two groups of false targets.

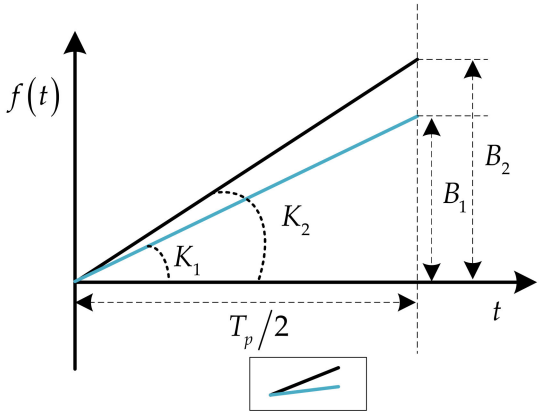

Figure 1. Sketch map of the instantaneous frequency of the twinning waveform.

According to the analysis in Section 2, the time delay sequence number corresponding to peak detection is determined by the number of copies of radar signals Q forwarded by jammers. Since the received mixed signals contain real target signals, the time delay sequence number of fake targets is $Q+1$. According to Equation (7), the jamming delay parameter is estimated as follows.

$$\hat{\tau}_q = (K_2 t_{d2}(q) - K_1 t_{d1}(q))/(K_2 - K_1) \tag{15}$$

In order to accurately estimate the jamming frequency parameters, it is necessary to construct the delay difference sequence based on the two-channel imaging results, as shown below.

$$\Delta t_d(q) = t_{d2}(q) - t_{d1}(q) \tag{16}$$

The estimated jamming frequency parameter is as follows based on the delay difference sequence.

$$\hat{f}_d = (K_1 K_2 \Delta t_d(q))/(K_2 - K_1) \tag{17}$$

4. Atomic Decomposition of Jamming Signals

Atomic decomposition theory is mainly used for adaptive approximation and decomposition of signals. Different atomic dictionaries are designed to achieve different characteristics of signals in the time-frequency domain [25]. Most atomic decomposition methods are based on the matching pursuit algorithm to solve, and the effect and efficiency of decomposition are closely related to the design of the atomic dictionary. When atomic dictionaries are close to each other and do not meet the sparse condition, the resolution of the matching pursuit decreases and the decomposition effect becomes worse.

Supposing that the target signal to be decomposed is $Q(t)$, there exists a function set $D = \{g_\eta(t)\}_{\eta \in \Pi}$ of the signal space and $\|g_\eta(t)\| = 1$. On this function set, the target signal can be expressed linearly by partial functions as follows:

$$Q'(t) = \sum_{\mathrm{m}=1}^{M} c_m g_{\eta m}(t) \tag{18}$$

where $Q'(t)$ is the best approximate signal of the target signal, $g_\eta(t)$ is the atom, the function set D is the atom dictionary or atom library, and c_m is the atom coefficient.

When the atoms in the atomic dictionary satisfy orthogonality, the atomic coefficients can be obtained directly as follows:

$$c_m = \langle g_{\eta m}(t), Q'(t) \rangle \tag{19}$$

where $\langle *, * \rangle$ is the inner product operation on that space. However, in practice, it is difficult to satisfy the orthogonality between atoms, so a generalized solution method, namely the matching pursuit method, is generally used to find the best atom. In each decomposition process, the best matching atom $g_{\eta 0}(t)$ is found in the dictionary according to the following criteria.

$$\left\langle g_{\eta 0}(t), Q(t) \right\rangle = \sup_{\gamma \in \Pi} \left| \left\langle g_{\eta}(t), Q(t) \right\rangle \right| \tag{20}$$

Through decomposition, the target signal can be expressed as follows:

$$Q(t) = \left\langle g_{\eta 0}(t), Q(t) \right\rangle g_{\eta 0}(t) + R^1 Q(t) \tag{21}$$

where $R^1 Q(t)$ is the residual signal, and then the same atomic decomposition operation is performed on the residual signal to find the best matching atom $g_{\eta 1}(t)$, with the following relations.

$$R^1 Q(t) = \left\langle g_{\eta 1}(t), Q(t) \right\rangle g_{\eta 1}(t) + R^2 Q(t) \tag{22}$$

The final decomposition expression of the signal was obtained after the above decomposition process was repeated M times.

$$Q(t) = \sum_{m=0}^{M-1} \left\langle g_{\gamma m}(t), R^m Q(t) \right\rangle g_{\gamma m}(t) + R^M Q(t) \tag{23}$$

In the jamming suppression algorithm proposed in this paper, the jamming signals in the mixed signals are decomposed into the optimized atomic dictionary to achieve the separation and elimination of jamming signals. Compared with the traditional complete dictionary in atomic decomposition, the atomic dictionary designed in this paper reflects the jamming characteristic parameters and achieves the separation of mixed signals while completing atomic decomposition.

By calculating the projection coefficients of atomic decomposition on different atom dictionaries, the accurate estimation of the mixed amplitude modulation coefficient $\{\mathbb{C}_q\}$ in the jamming model can be achieved. The commonly used atomic dictionaries include the Gabor atomic dictionary, Chirp atomic dictionary, and Chirplet atomic dictionary. The relevant literature shows that Chirplet can better decompose and fit linear frequency modulated (LFM) signals [25], and the mathematical expression is as follows.

$$g_{\eta}(t) = \frac{1}{\sqrt{s}} g\left(\frac{t-u}{s}\right) \exp\left(\mathrm{j}\left(\omega(t-u) + \frac{1}{2}\xi(t-u)^2\right)\right) \tag{24}$$

The atomic dictionary is determined by scale factor s, delay factor u, frequency shift factor ω, and frequency modulation slope factor ξ. In order to realize an efficient computation of the chirp signal decomposition, atomic dictionary parameter sets are often discretized rather than continuous. By the approximate optimal discretization of four continuous dictionary parameters, the atomic space is discretized to obtain a small but complete subset in the Hilbert space [26]. According to the discretization criterion in [26], the parameter set can be discretized to the following expression.

$$\eta = (s, u, \omega, \xi) = \left(\alpha^j, p\alpha^j \Delta u, k\alpha^{-j} \Delta\omega, l\alpha^{-2j} \Delta\xi\right) \tag{25}$$

Because the atomic dictionary is not sensitive to scale, in discrete design, $\alpha = 2$, $\Delta u = 0.5$, $\Delta\omega = \pi$, $\Delta\eta = \pi$, $0 < j \le \log_2 N$, $0 \le p \le N \cdot 2^{-j+1}$, $0 \le k < 2^{j+1}$, $0 \le l \le 2^{j+1}$, and N is the length of the signal. The design of atomic dictionary parameters based on the approximate optimal discrete method ensures the completeness of the dictionary, but each decomposition search time is long, resulting in a large computational burden and low

algorithm efficiency. Therefore, it is necessary to further optimize the design of dictionary parameter sets.

For the anti-jamming side, the initial parameters of the transmitted signal are known. Based on the analysis of the jamming model in Section 2, the frequency modulation slope of the jamming signal does not change. Therefore, the parameter set of the atomic dictionary does not need to search the frequency modulation slope, and the parameter set is simplified as follows:

$$\eta = (s, u, \omega, \xi) = \left(\alpha^j, p\alpha^j \Delta u, k\alpha^{-j} \Delta\omega, K\right) \tag{26}$$

All atoms in the dictionary have the same slope of the same frequency modulation as the transmitted signal. The optimal design of the delay factor and frequency shift factor is further discussed.

If the approximate optimal discrete method is directly adopted to design the parameter set range of the Chirplet atomic dictionary, the number of atomic dictionaries will be large, the decomposition efficiency will be low, the corresponding relationship with the components of jamming signals cannot be established, and the separation of jamming signals cannot be realized after the decomposition. In order to realize the one-to-one correspondence between the atomic dictionary and jamming parameters, the Chirplet atomic parameter set is defined as follows, based on the prior information estimated in Section 3, referring to the selection of optimal frequency in the adaptive atomic decomposition algorithm.

$$\eta = (s, u, \omega, \xi) = \left(\alpha^j, \hat{\tau}_q, \hat{f}_d, K_2\right) \tag{27}$$

After optimizing the atomic parameter set, the number of atomic dictionaries is equal to the number of copies of the forward target signal in the jamming signal and is the same as the number of false targets. Compared with the traditional over-complete atomic dictionary parameter set, the dictionary search range is greatly reduced, which improves the decomposition efficiency and achieves the effective separation of jamming signal atoms.

To sum up, a new smart jamming suppression algorithm is designed in this paper. Figure 2 shows a schematic diagram of the proposed algorithm. It first needs to transmit composite LFM signals to obtain two sets of jamming imaging results. Because of the difference in chirp rate between the twinning waveform signal and the original target signal, the position of the jamming false target group moves. Then, the estimators of the jamming delay sequence and jamming frequency sequence are constructed by using the time delay sequence corresponding to the peak positions of two false targets to achieve accurate estimation. The parameter set of the Chirplet atomic decomposition dictionary is optimized based on the estimated jamming delay sequence and jamming frequency sequence. The optimal decomposition of jamming signals based on the atomic dictionary is obtained by the matching pursuit algorithm, and the projection coefficients of different jamming atoms are obtained.

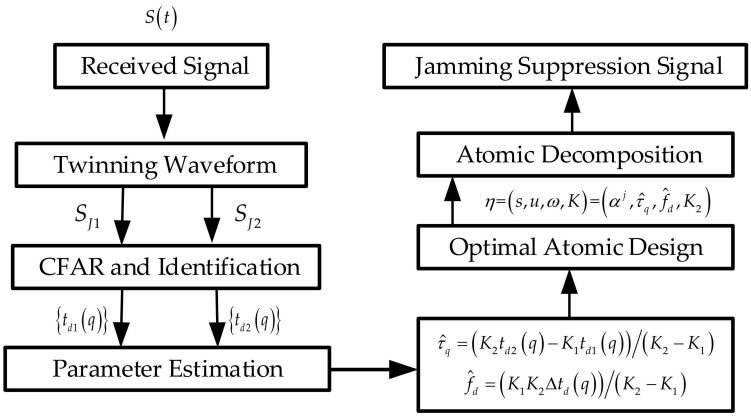

Figure 2. Jamming suppression flowchart.

The atomic decomposition process is equivalent to the accurate reconstruction process of the smart convolution jamming signal, and the remaining signal after the final decomposition is the target signal after jamming suppression. The proposed method can greatly improve the efficiency of atomic decomposition and jamming suppression.

The steps of jamming suppression are described below.

Step 1: Combined with sampling frequency and pulse width, the composite LFM signal was designed, and the two groups of jamming signals, S_{J1} and S_{J2}, were stored by the recombination of odd and even sequences.

Step 2: Two groups of false target distributions are obtained by designing different reference signals for imaging processing based on different frequency modulation slopes, K_1 and K_2, of odd and even sequences. The peak position of the imaging results is detected, and the time delay sequence of the false target, $\{t_{d1}(q)\}$ and $\{t_{d2}(q)\}$, are obtained.

Step 3: The estimators of jamming delay parameters $\hat{\tau}_q$ are established as $\hat{\tau}_q = (K_2 t_{d2}(q) - K_1 t_{d1}(q))/(K_2 - K_1)$. Then, the delay difference sequence $\{\Delta t_d(q)\}$ is constructed as $\Delta t_d(q) = t_{d2}(q) - t_{d1}(q)$, and finally the estimators of the jamming frequency parameter $\hat{f}_d$ are established as $\hat{f}_d = (K_1 K_2 \Delta t_d(q))/(K_2 - K_1)$.

Step 4: In order to obtain a better frequency range for dictionary design and signal decomposition, jamming signals with higher slopes of LFM are selected for decomposition. The original undecomposed signal S_{J2} is defined as residual signal $R^0Q(t)$, and the initial Chirplet atomic dictionary $D_0 = \{g_\eta(t)\}_{\eta \in \Pi_0}$ is designed by $\hat{\tau}_q$ and $\hat{f}_d$, and the corresponding parameter set is $\eta = (s, u, \omega, K) = \left(\alpha^j, \hat{\tau}_q, \hat{f}_d, K_2\right)$.

Step 5: The optimal matching atom $g_\eta^{\text{opt}}(t)$ is obtained by searching in the initial atom dictionary, and the projection coefficient $\left\langle R^0Q(t), g_\eta^{\text{opt}}(t) \right\rangle$ and residual jamming signal $R^1Q(t)$ under the optimal matching atom are obtained.

Step 6: Repeat step 5 to update the residual signal and search again based on the atomic dictionary until the optimal matching atom traverses the entire atomic dictionary and stops decomposition. The residual signal after decomposition is the target signal after jamming suppression, and the result after jamming suppression is obtained through imaging processing.

The specific algorithm is shown in Algorithm 1.

Algorithm 1. Atomic Dictionary Parameter Optimization Decomposition

Input: the sampling frequency of the signal f_s, the pulse width T_p, the chirp rate of twinning waveform K_1 and K_2, mixed jamming signal S_{J1} and S_{J2}
Output: The target signal after jamming suppression
1. Determine the time delay sequence of the false target $\{t_{d1}(q)\}$ and $\{t_{d2}(q)\}$ by imaging results;
2. Calculate the jamming delay parameters by $\hat{\tau}_q = (K_2 t_{d2}(q) - K_1 t_{d1}(q))/(K_2 - K_1)$;
3. Calculate the jamming frequency parameters by $\Delta t_d(q) = t_{d2}(q) - t_{d1}(q)$ and $\hat{f}_d = (K_1 K_2 \Delta t_d(q))/(K_2 - K_1)$;
4. Design the optimization atomic dictionary by $\eta = (s, u, \omega, K) = \left(\alpha^j, \hat{\tau}_q, \hat{f}_d, K_2\right)$ and decompose the mixed jamming signal;
5. If all the atoms are reconstructed, stop the decomposition and output the signal without jamming; otherwise return to 4.

5. Simulations

In this section, the validity and performance of the smart noise jamming suppression method is carried out by simulations. The radar transmitted signal is a LFM signal and the bandwidth is 10 MHz, which means the range resolution is 15 m, pulse width is 20 μs, and sampling frequency is 25 MHz. The time domain and spectrum of the transmitted original signal without jamming are shown in Figure 3.

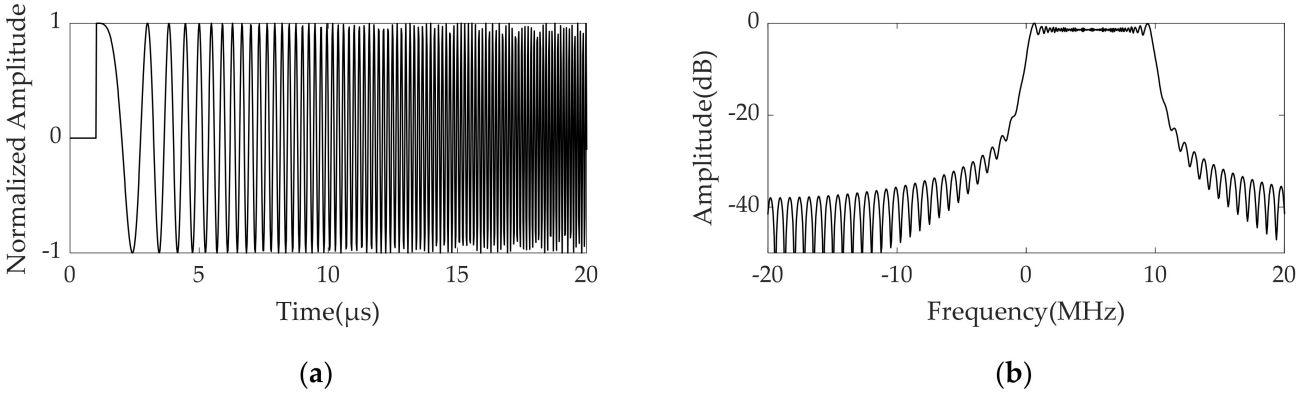

Figure 3. Time domain and frequency domain distribution of the LFM signal. (**a**) Time domain; (**b**) frequency domain.

The number of the jamming delay sequence introduced by the jammer is five, and the corresponding sequence value is {1 μs,2 μs,3 μs,4 μs,5 μs}. In the jamming signal, the noise sequence convolved with the target signal is a discrete complex Gaussian white noise sequence with unit variance. The time domain diagram and spectrum diagram of the received jamming signal are shown in Figure 4.

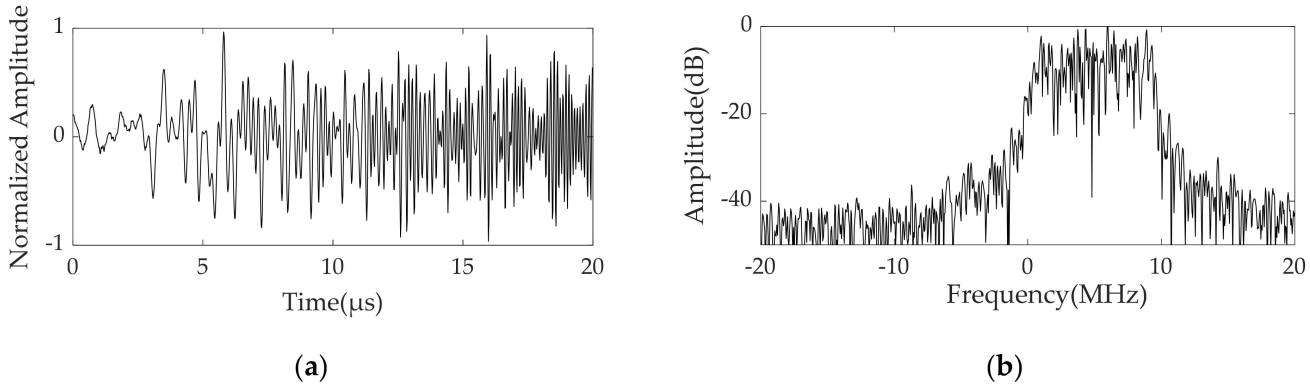

Figure 4. Time domain and frequency domain distribution of jamming signal. (**a**) Time domain; (**b**) frequency domain.

It can be seen from Figure 4 that the jamming signal presents a distribution similar to a Gaussian white noise sequence in the time domain, while in the frequency domain, it is modulated with Gaussian white noise within the effective frequency band. Compared with the traditional noise jamming, the energy of the forwarded target signal is effectively utilized and the energy power of the jammer is improved.

The imaging results of jamming signals and original target signals obtained by the pulse compression imaging algorithm are shown in Figure 5. If there is only the jamming delay sequence, the distribution of fake targets can only be located on one side of the real target, as shown in Figure 5a, which cannot effectively cover the real target. It is necessary to introduce the appropriate jamming frequency sequence to distribute fake targets evenly on both sides of the real target, so as to achieve a better effect of deception and jamming. The jamming frequency introduced by the jammer is 3MHz. The jamming effect is shown in Figure 5b.

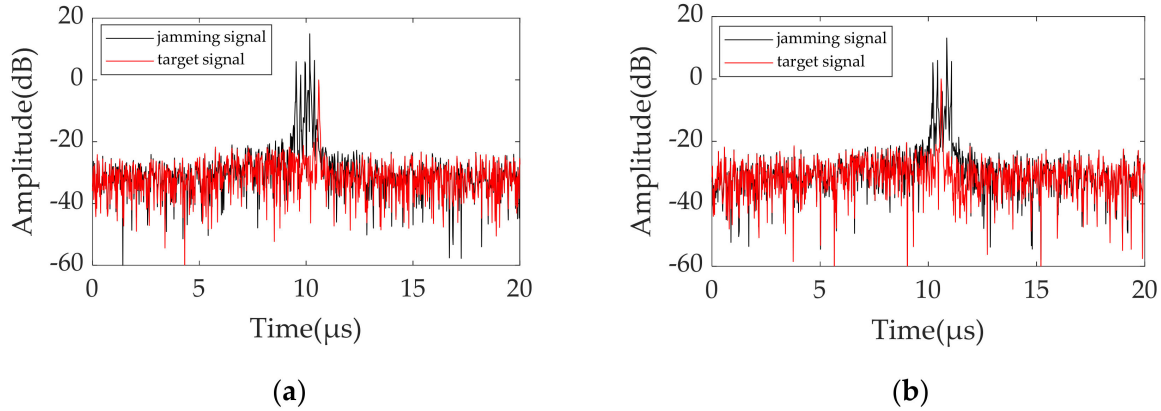

Figure 5. Pulse compression imaging results of the LFM signal and jamming signal. (**a**) Jamming results with only time delay sequence; (**b**) jamming results with frequency delay sequence.

5.1. Analysis of Smart Noise Convolution Jamming Effect under Different Jamming Time Delay and Frequency Sequence Combination

The design of the delay sequence needs to be combined with the pulse width of the transmitted signal. In order to quantitatively represent the influence of different jamming delay sequences on the false target position caused by the convolution noise jamming, two groups of jamming delay sequences with different intervals are designed, as shown in Table 1.

Table 1. Jamming delay sequence.

Jamming Delay Sequence Number N_t	**1**	**2**	**3**	**4**	**5**
Jamming delay $\{\tau_{q1}\}$ (μs)	1	3	5	7	9
Jamming delay $\{\tau_{q2}\}$ (μs)	3.1	3.2	3.3	3.4	3.5

Due to the difference in the spacing between the two groups of jamming delay sequences, the density of the fake target distributed near the real target is also different. The imaging results obtained by using the pulse compression imaging algorithm are shown in Figure 6. Because the range of the time delay sequence cannot exceed the pulse width of the transmitted signal, the movement range of false targets is limited. A wider range of adjustment is achieved by introducing frequency modulation.

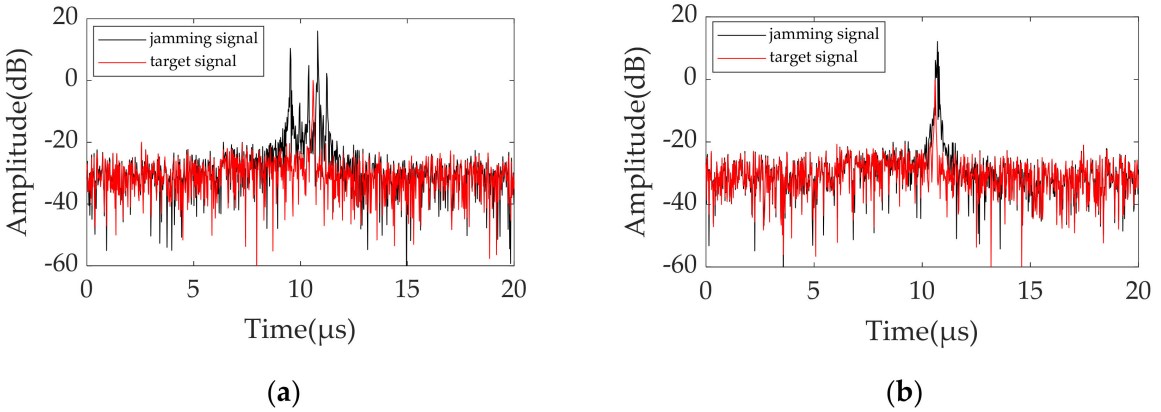

Figure 6. Comparison of imaging results with different jamming delay sequences. (**a**) Jamming delay sequences $\{\tau_{q1}\}$; (**b**) jamming delay sequences $\{\tau_{q2}\}$.

At the same time, when the jamming delay sequence is fixed, different jamming frequency sequences can be designed to adjust the spatial position of the fake target. Two

groups of jamming frequency sequences with different intervals are designed, as shown in Table 2. The imaging results are shown in Figure 7, so that the spatial position of the fake target can be adjusted freely in a wider range.

Table 2. Jamming frequency sequence.

	1	2	3	4	5
Jamming delay$\{f_{q1}\}$ (MHz)	0	4	6	8	10
Jamming delay$\{f_{q2}\}$ (MHz)	0	5	10	15	20

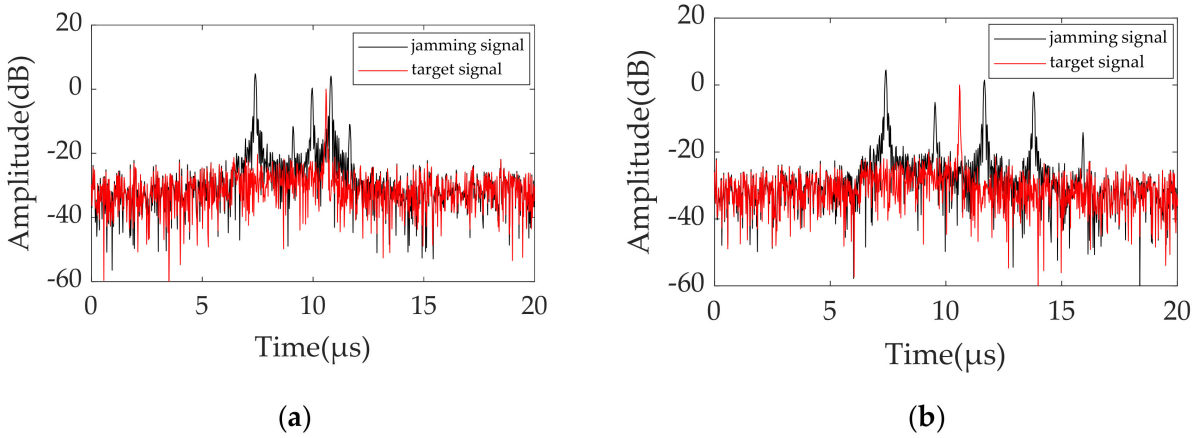

Figure 7. Comparison of imaging results with different jamming frequency sequences. (**a**) Jamming frequency sequences $\{f_{q1}\}$; (**b**) jamming frequency sequences $\{f_{q2}\}$.

5.2. Comparison of Jamming Suppression Performances of Different Atomic Dictionary Sets

In order to measure the performance of the atomic decomposition algorithm, it is necessary to analyze the change of the residual signal energy ratio with different atomic dictionaries with decomposition times. After the k-th decomposition, the residual signal energy ratio is $R_{SNR}(k)$.

$$R_{SNR}(k) = (E_{SNR}(k)/E_S) \times 100\% \tag{28}$$

where k is the decomposition times, $E_{SNR}(k)$ represents the remaining signal energy after k times of decomposition, and E_S represents the energy of the original undecomposed signal.

The jamming to signal ratio (*JSR*) and signal to noise ratio (*SNR*) are defined as follows:

$$JSR = \int_{-\infty}^{\infty} |J(t)|^2 dt / \int_{-\infty}^{\infty} |s(t)|^2 dt \tag{29}$$

$$SNR = \int_{-\infty}^{\infty} |s(t)|^2 dt / \int_{-\infty}^{\infty} |n(t)|^2 dt \tag{30}$$

where $s(t)$ is the target signal, $J(t)$ is the jamming signal, and $n(t)$ is additive Gaussian white noise with zero mean.

The number of the jamming delay sequence and jamming frequency sequency introduced by the jammer are five, which is same with Section 5.1. Next, the jamming decomposition performance is analyzed when the jamming delay sequence is $\{\tau_{q2}\}$ and the jamming frequency sequence is $\{f_{q2}\}$, where SNR is 20 dB, and JSR is 14 dB to ensure that the energy of each jamming component is consistent with the target signal.

Conclusions can be drawn from Figure 8 as follows. Compared with the traditional Chirplet atomic dictionary and the atomic dictionary in [21], the optimized atomic dictionary only needs five iterations of effective decomposition and the residual energy ratio can be reduced to a lower level, while the traditional atomic dictionary and the atomic

dictionary in [21] needs more than 30 iterations of decomposition to achieve the same energy decomposition. Therefore, the atomic decomposition algorithm proposed in this paper can achieve the rapid decomposition of jamming signals. It not only ensures the effective separation of jamming signals, but also achieves higher decomposition efficiency.

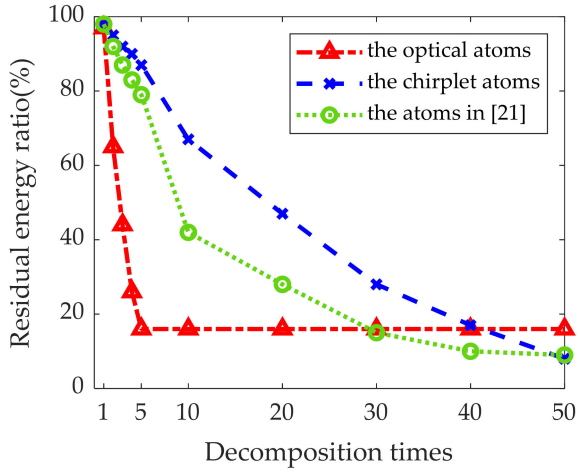

Figure 8. Variation curves of residual energy ratio after decomposition with different atomic dictionaries.

The influence of different SNRs on the suppression effect of atomic dictionary decomposition is simulated. Gaussian white noise with SNR of −5 dB, 0 dB, 5 dB, 10 dB, 15 dB, and 20 dB are added to the target signal and JSR is 14 dB. As observed in Figure 9, with the increase in noise power, the residual energy ratio becomes larger under the same decomposition times, especially when the SNR is −5 dB. In general, after five times of decomposition, all residual signal energies are reduced to below 40%, and the jamming signal is suppressed under different SNRs. Since the residual noise signal cannot obtain pulse compression gain in the imaging results, the detection of the real target signal is not affected. The above experiments demonstrate the effectiveness of the proposed method under different SNR conditions.

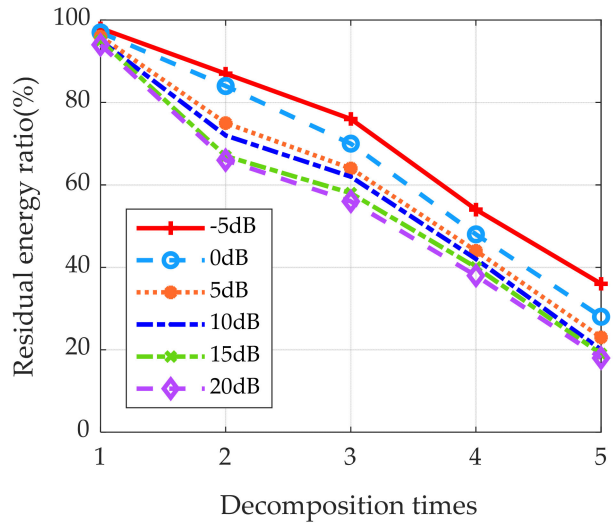

Figure 9. Variation curves of residual energy ratio after atomic dictionary decomposition under different SNR conditions.

Figure 10 shows the comparison of the amplitude distribution of imaging results of original mixed signals without jamming suppression and signals after five times of matched pursuit decomposition of two different atomic dictionaries, where SNR is 20 dB and JSR is 14 dB. The solid green line represents the result of jamming suppression by the

method in [21] and the solid red line represents the result of jamming suppression by the method proposed in this paper. As observed from this, the amplitude corresponding to the false targets' positions generated by the jamming signal are reduced by at least 20 dB after suppression with our proposed method. However, the amplitude of the false targets by the method proposed in [21] is still partially residual, which will affect the detection of real targets. Therefore, by comparison of imaging results, the interference suppression method in this paper can achieve more effective smart noise jamming suppression with limited decomposition times.

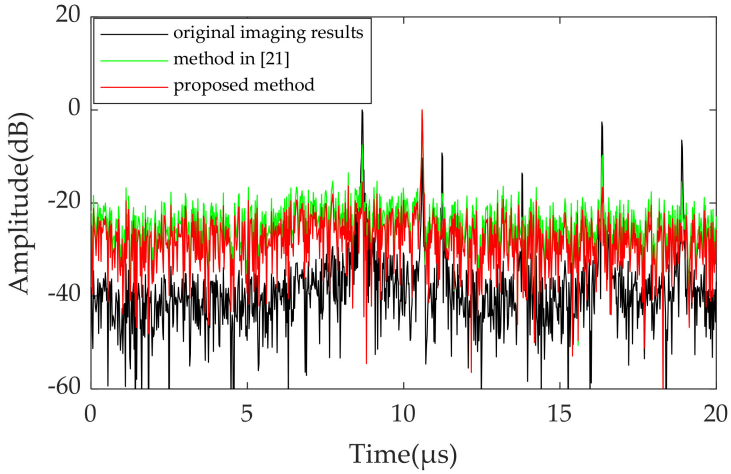

Figure 10. Comparison of image results before and after jamming suppression with different methods.

Based on above simulations, it can be observed that:

(1) Smart noise jamming can achieve different deception effects by dynamically adjusting the interference parameters, including the delay sequence and jamming frequency sequence, which brings great challenges to suppression. Therefore, it is necessary to study efficient suppression methods for different jamming effects.

(2) Since the spatial distribution of the false targets is simultaneously determined by two key interference parameters, it is necessary to provide additional information and establish additional equations to estimate the two independent parameters. In order to solve the above problems, the twinning waveform design is introduced to realize the independence of two interference parameters without increasing the complexity of the algorithm.

(3) The method of atomic dictionary decomposition can effectively eliminate the jamming signal components, but the existing atomic dictionary design is redundant and the decomposition efficiency is not high. By optimizing the design of dictionary parameters, one-to-one correspondence between the interference signal components and atomic dictionary is realized, which improves the decomposition efficiency. The effectiveness of the proposed method is verified under different SNR conditions.

(4) When the spatial position variation of the two jamming results is less than the range resolution of the radar, or the jamming effect is blanket jamming in real-world situations, the linear mapping relationship cannot be established and radar resolution needs to be improved to realize the effective separation of the aliased false targets. Different threshold filtering operations can be carried out before and after jamming suppression in view of the noise with large energy in the actual radar system.

6. Conclusions

In this paper, the suppression method of convolutional smart noise jamming is studied. The independent estimation of the jamming parameters is realized by using the dual-channel twinning waveform design, and the dictionary in atomic decomposition is optimized to realize the one-to-one correspondence between the atomic dictionary and the jamming components, which improves the accuracy and efficiency of the matching

pursuit algorithm and completes the accurate reconstruction and effective suppression of the jamming signal. This paper provides a new method of jamming suppression, which provides a new solution for the future research on the dense false target deception jamming suppression method. However, when the smart noise jamming is transformed into the blanket jamming effect, the jamming characteristic parameter estimation method proposed in this paper will become invalid. Therefore, further research should focus on surmounting this shortcoming.

Author Contributions: Z.L. and Q.Z. proposed the method and designed the experiments; Q.Z. and K.L. coordinated reading, analyzing, and categorizing the articles reviewed in this study; Z.L. and K.L. analyzed the data; Z.L. performed the experiments and wrote and revised the paper. All authors have read and agreed to the published version of the manuscript.

Funding: This research was funded by the National Natural Science Foundation of China, grant number 61631020 and 61971434.

Data Availability Statement: Not applicable.

Acknowledgments: The authors would like to thank the handling editor and the anonymous reviewers for their valuable comments and suggestions for this paper.

Conflicts of Interest: The authors declare no conflict of interest.

References

1. Berger, S. Digital radio frequency memory linear range gate stealer spectrum. *IEEE Trans. Aerosp. Electron. Syst.* **2003**, *39*, 725–735. [CrossRef]
2. Jin, S.S.; Wang, C.Y.; Li, X.; Zhang, X.F.; Sun, Y.X. Method for Active Radar Seeker to Suppress Convolution Modulation Smart Jamming. *Appl. Mech. Mater.* **2014**, *568–570*, 212–217. [CrossRef]
3. Youssef, A.; Driessen, P.F.; Gebali, F.; Belaid, M. Performance evaluation of time compression overlap-add radar systems based on order-statistics CFAR under convolution noise jamming. In Proceedings of the 2017 IEEE Pacific Rim Conference on Communications, Computers and Signal Processing (PACRIM), Victoria, BC, Canada, 21–23 August 2019; pp. 1–6. [CrossRef]
4. Xiao-Yang, X.U.; Bao, Y.X.; Zhou, H.Y. Technology of Smart Noise Jamming Based on Convolution Modulation. *Mod. Radar* **2007**, *29*, 28–31.
5. Guo, J.; Wang, X.; Wang, X.; Si, J.; Zhang, W. New smart noise jamming of radar signal frequency modulation. *J. Xidian Univ.* **2013**, *40*, 155–160. [CrossRef]
6. Han, B.; Yang, X.; Wu, X.; Li, S. Smart noise jamming suppression method based on fast fractional filtering. *J. Eng.* **2019**, *2019*, 6201–6205. [CrossRef]
7. Chen, W.; He, Z.; Yan, Y. Electronic counter-countermeasures scheme for smart noise jamming using orthogonal diversity. *J. Natl. Univ. Def. Technol.* **2018**, *40*, 107–113. [CrossRef]
8. Ren, J.; Wang, P. Novel smart noise jamming suppression method based on smeared spectrum. *Prog. Electromagn. Res. Lett.* **2017**, *67*, 81–88. [CrossRef]
9. Ren, J. Jamming Suppression Technology in LFM Radars. Ph.D. Dissertation, University of Science and Technology of China, Hefei, China, 2017.
10. Yan, Y.; Li, M.; Lu, Y. Multi-Feature-Based identification of smart noise jamming. *Radar Sci. Technol.* **2013**, *11*, 455–461. [CrossRef]
11. Chen, W.; Zhang, J.; Xie, W.; Wang, Y. Research on smart jamming signal model and suppression method for airborne phased array radar. *Syst. Eng. Electron.* **2021**, *43*, 343–350. [CrossRef]
12. Yeste-Ojeda, O.A.; Grajal, J.; Lopez-Risueno, G. Atomic decomposition for radar applications. *IEEE Trans. Aerosp. Electron. Syst.* **2008**, *44*, 187–200. [CrossRef]
13. Liu, J.; Wang, K.; Liu, X.; Yu, W. Optimal waveforms design for radar imaging based on atomic decomposition RCS charac-teristics of target. In Proceedings of the IEEE 2012 International Waveform Diversity & Design Conference (WDD), Kauai, HI, USA, 22–27 January 2012.
14. Gao, Y.; Wang, K.; Liu, X. Atomic decomposition-based SAR imaging. In Proceedings of the 2011 IEEE International Geoscience and Remote Sensing Symposium, Vancouver, BC, Canada, 24–29 July 2011.
15. Yeste-Ojeda, O.; Grajal, J. Atomic Decomposition based detector for denoising in ISAR imaging. In Proceedings of the 14th European Signal Processing Conference, Florence, Italy, 4–8 September 2006.
16. Wang, X.; Liu, J.; Meng, H.; Liu, Y. Novel atomic decomposition algorithm for parameter estimation of multiple superimposed Gaussian chirplets. *IET Radar Sonar Navig.* **2011**, *5*, 854–861. [CrossRef]
17. Lopez-Risueno, G.; Grajal, J. Multiple signal detection and estimation using atomic decomposition and EM. *IEEE Trans. Aerosp. Electron. Syst.* **2006**, *42*, 84–102. [CrossRef]

18. Sun, M.; Tang, B. Feature extraction of radar deceptive-jamming signal based on atomic decomposition. *Chin. J. Radio Sci.* **2008**, *3*, 550–554. [CrossRef]
19. Chen, X.; Zhang, X.; Yang, J.; Sun, M. How to overcome basis mismatch: From atomic norm to grid less compressive sensing. *Acta Autom. Sin.* **2016**, *42*, 335–346. [CrossRef]
20. Zhou, Y.; Wang, X.; Tian, Y.; Zhou, D. A novel time-frequency atomic dictionary for radar intra-pulse modulation signal sparse representation. In Proceedings of the 2015 Asia-Pacific Microwave Conference (APMC), Nanjing, China, 6–9 December 2015; pp. 1–3. [CrossRef]
21. Zhang, Z.; Wu, Y.; Ren, J.; Dong, K. Smart noise jamming suppression by using atomic decomposition. In Proceedings of the 2017 3rd IEEE International Conference on Computer and Communications (ICCC), Chengdu, China, 13–16 December 2017; pp. 1377–1380. [CrossRef]
22. Sun, M.; Tang, B. Suppression of smeared spectrum ECM signal. *J. Chin. Inst. Eng.* **2009**, *32*, 407–413. [CrossRef]
23. Hao, Z.; Yu, W.; Chen, W. Recognition method of dense false targets jamming based on time-frequency atomic decomposition. *J. Eng.* **2019**, *2019*, 6354–6358. [CrossRef]
24. Liu, Z.; Zhang, Q.; Luo, Y.; Li, R. A smeared spectrum interference suppression method based on twinwaveform design. *Acta Aeronaut. Astronaut. Sin.* **2022**, *43*, 324947. [CrossRef]
25. Guo, P.; Wang, X.; Chen, S.; Wang, F. Non-linear frequency modulated signal decomposition based on the improved chirplet time-frequency atom. *J. Xidian Univ.* **2018**, *45*, 123–128. [CrossRef]
26. Bultan, A. A four-parameter atomic decomposition of chirplets. *IEEE Trans. Signal Process.* **1999**, *47*, 731–745. [CrossRef]